Transfer functions in a karst watershed using correlation and spectral analyses

Case of the *Coulazou* watershed, *Aumelas-Thau* karst system, South of France

Bailly-Comte Vincent, Jourde Hervé, Pistre Séverin

Laboratoire HydroSciences Montpellier, Maison des Sciences de l'Eau, UM2, Montpellier – France

+33 4 67 14 90 44, bailly@msem.univ-montp2.fr

Abstract

This work aims at assessing rainfall/runoff and runoff/runoff relationships in a karst watershed. Rain gauges and gauging stations allow estimating River flow which reaches and leaves the karst aquifer. Correlation analyses are firstly used to describe rainfall/runoff transfer functions upstream and downstream from the karst aquifer. Then, correlation and spectral analyses applied to a runoff/runoff relationship are used to understand how flood waves in the River are modified through the karst aquifer. It is shown that frequency response is a suitable data analysis tool which highlights various processes occurring on different time scale: surface flow routing, exceeding of the infiltration rate of the karst drainage network and karst contribution to surface flows.

I. Introduction

A lot of works have used linear input-output models for karst aquifer analysis (e.g. Bailly-Comte et al., 2008a; Bailly-Comte et al., 2008b; Dreiss, 1983; Larocque et al., 1998; Mangin, 1984; Massei et al., 2006; Padilla and Pulido-Bosch, 1995; Rahnemaei et al., 2005) or for karst flows simulation (Labat et al., 2000a; Long and Derickson, 1999). It is now admitted that karst systems have a non-linear and non stationary behaviour (e.g. Bailly-Comte et al., 2008a; Bailly-Comte et al., 2008b; Jukic and Denic-Jukic, 2004; Labat et al., 2000a; Massei et al., 2006), which implies that karst spring discharge, and more generally karst flows do not simply result from convolution of a non time dependent transfer function and a rainfall time series.

As a consequence some authors have proposed alternative approaches based on a combination of two linear transfer functions (composite transfer functions) dedicated to so called slow and quick flows components (Denic-Jukic and Jukic, 2003) or on non-linear kernel function (Jukic and Denic-Jukic, 2006; Labat et al., 2000b). Simple linear input-ouput models give however interesting results when applied to the description of time series structures, which may constitute a first step to karst aquifer modelling (Bailly-Comte et al., 2008b; Mangin, 1984). In this case the input-output model is only used to describe the system and no output simulation is attempted. These linear input-output models do not need information about the internal structure of aquifers and mathematical relations between input and output time series are derived without applying physical laws (Denic-Jukic and Jukic, 2003). As a result, Time Series Analysis (TSA) applied to karst flows gives information on the structure and the behaviour of a karst aquifer in an indirect way by interpreting the induced effect on the output of an input variation. Different types of measurements may be used as input and/or output: rainfall, spring discharge, runoff, water level, temperature, turbidity, electrical conductivity etc., but the main difficulty of simple input-output models comes from the choice of bivariate time series which are not influenced by a third one.

This paper deals with the genesis and the transfer of surface flows on karst watersheds, especially in case of karst aquifers with allogenic stream, that is stream which originates in a non karst watershed or in a karst watershed from another karst system. During floods the karst aquifer is thus partly fed by an allogenic stream and thus 3 combinations of rainfall runoff time series are available for bivariate analyses: (i) the rainfall/runoff relationship of the allogenic stream using a gauging station upstream from the karst aquifer, (ii) the rainfall/runoff relationship using a gauging station downstream from the karst aquifer and (iii) the runoff/runoff relationship using these two gauging stations. In the following, *upstream watershed* refers to the watershed of the allogenic stream, Q_1 represents the station which

gauges runoff in the allogenic stream as it reaches the karst aquifer and Q_2 is the second station which gauges the runoff in the river downstream from the karst aquifer (Fig. 1).

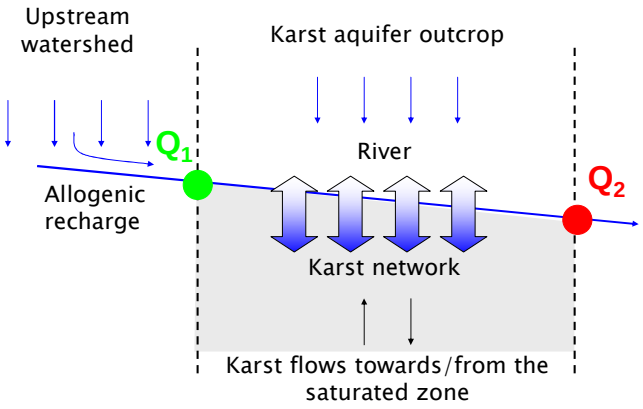

Fig. 1: Karst/River interaction in case of allogenic stream

Runoff in Q_2 accounts for Karst/River exchanges (Bailly-Comte et al., 2008b), including water losses through swallow holes and karst springs discharge.

II. Methods

The study is done at the flood event time scale which allows (i) considering hydrological processes as almost time invariant phenomena and (ii) analysing the input-output transformation according to the initial hydrogeologic conditions. The Jenkins and Watts method (1968) is used to analyse transfer functions for each bivariate time series.

Covariance and correlation analyses: Transfer function in the time domain

Pairs of n length time series $x_i(t)$ and $x_j(t)$ are selected to compute auto- and cross covariance coefficients $Cx_ix_j(k)$, i=1,2 and j=1,2 where k is the time lag. Computations are done using the following auto- and cross covariance coefficient (acvf and ccvf) estimates (1):

$$\begin{aligned} &C_{x_i x_j}(k) = \frac{1}{n} \times \sum_{1}^{n-k} (x_{i(t)} - \bar{x}_i) \times (x_{j(t+k)} - \bar{x}_j) \quad k \geq 0 \\ &C_{x_i x_j}(k) = C_{x_j x_i}(-k) \quad k < 0 \\ &acvf : i = j \\ &ccvf : i \neq j \end{aligned} \tag{1}$$

Results are generally normalised using (2) so that acvf and ccvf become auto- and cross correlation (acf and ccf) functions. Correlation coefficients rx_ix_j (k), i=1,2 and j=1,2 are given by (2).

$$r_{x_i x_j}(k) = \frac{C_{x_i x_j}(k)}{\sqrt{C_{x_i x_i}(0) \times C_{x_j x_j}(0)}} \tag{2}$$

Correlation analyses show how correlated are two time series for increasing time lag k; the bivariate time series can be identical (auto-correlation) or not (cross correlation). Estimates of acf and ccf versus the lag k are shown on a graph called respectively correlogram and cross correlogram. They are supposed to be valid for k=m<n/3 (Mangin, 1984), where m is the truncation point.

First conclusions about trends, memory effects and periodic structure of time series may be given by analysing shapes of correlograms while cross correlogram gives information about the response of the input-output system (Mangin, 1984). The cross correlation function is indeed the data analysis tool for the identification of transfer function (Box et al., 1994). If the input time series is a realization of a random process, the corresponding correlogram should be null for all lags k except for k=0 where the acf is always 1. In this case, assuming a Linear Time Invariant (LTI) process, the cross correlogram

gives an image of the transfer function of the system. The latter is also called the impulse response of the system and can be used to compute the output time series by convolution with the input time series. First order differenced time series are thus often used to remove trends in order to deal with modified times series representative of an almost random process (Jenkins and Watts, 1968). First order differenced time series are calculated for an *x* time series using (3).

$$diff(x_t) = x_t - x_{t-1} \quad t > 1 \tag{3}$$

Correlation analyses are also used as a first step for spectral analysis. Results and conclusions given by correlation analyses in the time domain can also be given in the frequency domain using the Fourier transform of the auto and cross covariance estimates (Eqs 1 and 2).

Spectral analyses: Transfer function in the frequency domain

This section deals with the frequency-domain description of bivariate time series. Fourier transform of acvf gives the Power Spectral Density (PSD) of the time series. PSD allows analysing the structure of a time series in a different way since it describes the frequency contents and intensities of the time series. In other words, it gives the decomposition of the sample variance with frequency and thus shows how the variance of the time series is distributed according to frequencies. Trends (contents at low to 0 frequencies) and periodic structures (peak on the spectral plot) are thus highlighted. The smoothing of spectral estimates (5) is determined by the choice of the window function w(k) (Jenkins and Watts, 1968). The Tukey (or Hanning) window is widely used in various sciences for its good spectral properties and has thus been chosen for this study to minimize sampling and truncation errors (4). PSD estimate is in fact the cosine transform of the estimate of acvf since the latter is an even function (5).

$$w(k) = \frac{1}{2} \times \left(1 + \cos\left(\frac{k\pi}{m}\right)\right) \quad |k| \le m, \text{m is the truncation point} \tag{4}$$

$$PSD_i(f) = 2 \times \left(C_{x_i x_i}(0) + 2 \times \sum_{k=1}^{m-1} C_{x_i x_i}(k) \times w(k) \times \cos(2\pi f k)\right) \text{ where } f = \frac{j}{2m}, j = 0,..,m \tag{5}$$

The Fourier transform of the ccvf gives a complex cross power spectrum C_{12} since ccvf is an odd function. As a result, 4 spectral functions can be given: (i) the cospectrum (real part, L_{12}), (ii) the quadrature spectrum (imaginary part, Q_{12}) and, in the complex form, (iii) the cross amplitude spectrum (A_{12}) and (iv) the phase spectrum (Φ_{12}). Spectral estimates are computed using the discrete Fourier transform proposed by Jenkins and Watts (1968) with the Tukey window function (4):

$$L_{12}(f) = 2 \times \left(C_{x_1 x_2}(0) + \sum_{k=1}^{m-1} \left(C_{x_1 x_2}(k) + C_{x_2 x_1}(k)\right) \times w(k) \times \cos(2\pi f k)\right) \tag{6}$$

$$Q_{12}(f) = 2 \times \sum_{k=1}^{m-1} \left(C_{x_1 x_2}(k) - C_{x_2 x_1}(k)\right) \times w(k) \times \sin(2\pi f k) \tag{7}$$

$$A_{12}(f) = \sqrt{Q^2{}_{12}(f) + L^2{}_{12}(f)} \tag{8}$$

The cross amplitude spectrum shows if frequency components in the input time series are associated with large or small amplitudes at the same frequency in the other series (Jenkins and Watts, 1968).

$$\Phi_{12}(f) = \arctan\left(-\frac{Q_{12}}{L_{12}}\right); \quad -\pi < \Phi_{12} \le \pi$$
$$\Delta t(t) = -\frac{\Phi_{12}}{2\pi f} \tag{9}$$

Phase spectrum shows if frequency components in the input time series lag or lead the components at the same frequency in the output time series; the phase delay Δt is computed using (9). All these estimates (Eqs. 5 to 9) are used to describe time series in the frequency domain. Moreover, spectral analyses allow expressing the frequency response H_{12} of the system, which is the transfer function of the system expressed in the frequency domain. The frequency response is thus equivalent to the impulse response in the frequency domain. Assuming that the input/output system is a LTI system and

considering that convolution in the time domain is simply a multiplication in the frequency domain, H_{12} may be written using PSD_1 and the cross power spectrum C_{12} (10):

$$H_{12}(f) = \frac{C_{12}}{PSD_1} = \frac{A_{12}}{PSD_1} \times e^{-i\Phi_{12}} = G_{12} \times e^{-i\Phi_{12}} \text{ where } G_{12}(f) = \frac{A_{12}}{PSD_1} \tag{10}$$

Two spectra characterise the transfer function in the frequency domain; the phase spectrum Φ_{12} and the gain spectrum G_{12}. If the system is linear, then (11):

$$PSD_2(f) = PSD_1 \times G^2{}_{12} \tag{11}$$

A combination of (11) and (10) allows defining another function called the squared coherence function K^2_{12} (f), which is equal to one for a linear system. Whatever the nature of the system, the Cauchy–Schwarz inequality implies furthermore that K^2_{12} is less or equal to one.

$$K^2{}_{12}(f) = \frac{A^2{}_{12}}{PSD_1 \times PSD_2} \tag{12}$$

As a result K^2_{12} is a test function which shows if the output signal can be interpreted as a modification of the input signal through a LTI system. The larger K^2_{12} is for a given frequency f, the more closely related are the f components of the input and output signals (Yevjevich, 1972). In case of low coherence values, a non-linear behaviour and/or additional inputs have to be considered.

Bias in phase, coherency and gain estimator can be reduced by aligning the time series before computing the ccvf estimates (Jenkins and Watts, 1968). This is done by shifting the output time series by the lag for which the ccf is the highest, leading to a so-called non-delayed system. An approximate (100-α)% confidence intervals for gain and phase estimates is proposed by Jenkins and Watts (1968), where f is the upper 100(1-α)% point of the F (Fisher-Snedecor) distribution with 2 and υ-2 degrees of freedom, υ is the number of degrees of freedom associated with the smoothing of the output spectrum.

$$\begin{aligned} G_{12}(f) &= \tilde{G}_{12}(f) \times \left(1 \pm \sqrt{\frac{2}{\upsilon - 2} \times f_{2,\upsilon-2}(1-\alpha) \times \frac{1 - K^2{}_{12}(f)}{K^2{}_{12}(f)}}\right) \\ \phi_{12}(f) &= \tilde{\phi}_{12}(f) \times \left(1 \pm \sqrt{\frac{2}{\upsilon - 2} \times f_{2,\upsilon-2}(1-\alpha) \times \frac{1 - K^2{}_{12}(f)}{K^2{}_{12}(f)}}\right) \end{aligned} \tag{13}$$

The number of degree of freedom υ is calculated using (14), where b is the standardised bandwidth of the spectral windows used for the smoothing of the output spectrum, which is 4/3 for the Tukey window (Jenkins and Watts, 1968).

$$\upsilon = \frac{2 \times b \times n}{m + 1} \tag{14}$$

In the following, Rainfall/Runoff (R/Q) relationships will be analysed in the time domain while Runoff/Runoff (Q/Q) relationship is analysed both in the time and frequency domain. Bode gain and phase plots ($20\log G_{12}$ in dB and Φ_{12} in radians on a log-frequency axis) are used to show frequency response estimates. Single or multiple resonant frequencies which characterise the system are highlighted by Bode plots where the gain estimate shows a local maximum and the phase estimate decreases rapidly.

All the iterative calculations are done with a Microsoft Visual Basic for Applications (VBA) macro in Excel 2003. Fast Fourier Transform is commonly employed for spectral analysis since the computation algorithm is much more efficient, but it only works for series with lengths that are a power of 2. In the Jenkins and Watts procedure, the length of the spectral window and the frequency resolution are related to k and m, while FFT procedure needs zero padding techniques. The Jenkins and Watts method has been chosen since estimates are easy to compute and computational time is reduced in case of short length time series.

III. Case study

Study area and monitoring network

Near Montpellier, Southern France, the *Coulazou* temporary River crosses the *Aumelas Causse* where the karst aquifer outcrops (Jurassic limestones, Fig. 2).

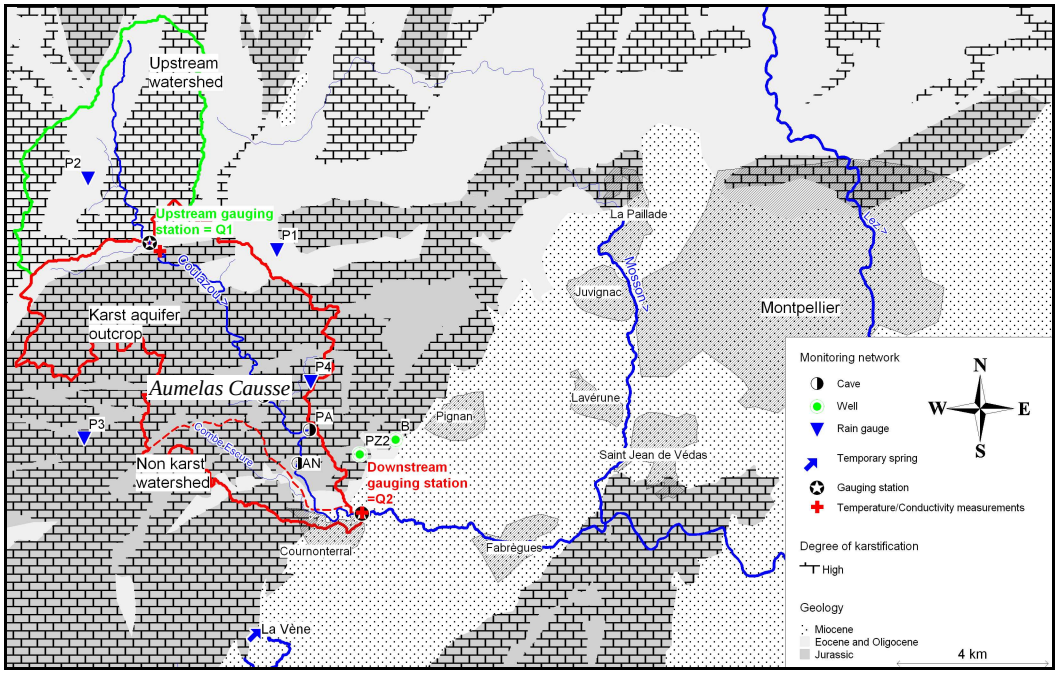

Fig. 2: Study area and monitoring network

A monitoring network (Fig. 2) has been settled for the Karst/River interactions assessment (Bailly-Comte et al., 2008a; Bailly-Comte et al., 2008b; Jourde et al., 2007) including (i) 4 rain gauges distributed over the 61 km² *Coulazou* watershed at a 5 min time step, (ii) surface flows measurements in the river upstream (Q_1) and downstream (Q_2) of the karst aquifer at a 5 min time step, (iii) water-level, temperature and electrical conductivity measurements in caves in the riverbed and wells near the river at a 10 min time step (Fig. 2).

This system constitutes a small scale experimental site to study the genesis and the transfer of surface flows before to focus on larger systems where floods hazards in karst area may have larger human and economic consequences.

Available data and previous hydrodynamic results

12 flood events have been analysed. Results and classification of Karst/River interactions are given for the 12 events in Table 1. Cumulative rainfall is given for the upstream watershed (R_{up}) by P2 (Fig. 2) and on the karst aquifer (R_{Karst}) by a weighted sum of P1, P3 and P4 (Fig. 2) using the Thiessen polygon method (Table 1). Hydrogeological information about the karst aquifer before the flood is also given (Initial water level in the karst aquifer, Table 1, (Bailly-Comte, 2008)).

Bivariate time series selection for transfer functions analysis

R/Q transformation characterises the "watershed" system while Q/Q transformation between Q_1 and Q_2 characterises the "Karst/River" system .The study of R/Q and Q/Q bivariate time series uses R_{up} vs Q_1 and R_{down} vs Q_2, where R_{down} is a combination of all rain gauges using the Thiessen polygon method on the whole watershed. Transfer functions are analysed in the time domain for each R/Q and Q/Q bivariate time series. Frequency response estimates are provided for the Q_1/Q_2 relationship for which gain and phase functions characterises the transformation of a runoff signal through a karst

watershed. Input/output time series are thus homogeneous (same unit) and the karst watershed between Q_1 and Q_2 stand for a filter which modifies the runoff, like an electronic system which amplifies or not the current.

Flood	Rainfall (mm)		Runoff Coeff. (%)		Initial water level in the karst aquifer	River reach classification between Q_1 and Q_2	
	R_{up}	R_{Karst}	Q_1	Q_2		Surf.W/Grd.W connexion	Direction of flows
1-Apr04	110	69	12	26	very high	Connected	Gaining
2-Oct04	122	28	8	3	low	Disconnected	Losing
3-Sept05	257	154	11	11	very low	Disconnected	Variably losing and gaining Mostly losing
4-Nov05	60	53	16	14	high	Connected	Variably losing and gaining Mostly gaining
5-Jan06	44	46	21	17	high	Connected	Gaining
6-Jan06	208	200	24	72	very high	Connected	Gaining
7-Sept06	145	141	1	2	very low	Disconnected	Variably losing and gaining Mostly gaining
8-Sept06	68	62	6	5	medium	Connected	Variably losing and gaining Mostly gaining
9-Sept06	31	13	10	0	high	Connected	Losing
10-Oct06	47	53	7	2	high	Connected	Variably losing and gaining Mostly losing
11-Oct06	nd.	11	-	-	very high	Connected	Variably losing and gaining Mostly losing
12-May07	48	54	6	5	medium	Connected	Variably losing and gaining Mostly gaining

Table 1: Hydrodynamic results and classification of Karst/River exchanges in the *Coulazou* watershed

Floods sample are subdivided into 2 groups and a comparison of transfer functions based on River classification (Table 1) is done.

Group A: Losing or variably gaining-losing with mostly losing reach, which are the floods 2, 3, 9, 10 and 11; R_{up} is unknown for the flood event 11.

Group B: Gaining or variably gaining-losing with mostly gaining reach, which are the floods 1, 4, 5, 6, 7, 8, and 12.

These 2 groups have been identified by previous Karst/River interaction studies between Q_1 and Q_2 (Fig. 2, (Bailly-Comte, 2008)). No information is available for groundwater-surface water interactions assessment in the upstream watershed. The same groups of floods are however used for the R_{up}/Q_1 relationship study so that comparisons between hydrologic processes occurring in the upstream watershed (R_{up}/Q_1) and in the whole watershed (R_{down}/Q_2 and Q_1/Q_2) can be done.

IV. Results and discussion

The number close to a curve is the name of the flood for each following graph.

R_{up}/Q_1 relationship

- Fig. 3-1 and Fig. 3-3 show results of auto correlations for the group A:

Rainfall correlograms show a high decrease for low time lags which means that no trend characterises the rainfall (input) time series (Fig. 3-1). The rainfall correlogram of the flood 3 is an ideal case since rainfall can be considered as a random process (Fig. 3-1, acf≈0 for k>0), while the other rainfall correlograms show some peaks which will influence the R_{up}/Q_1 cross correlation estimates. Both rainfall and runoff correlograms of the flood 3 increase for lags between 6h and 18h, but the runoff correlogram is much more damped. Indeed, runoff correlograms show that short term rainfall fluctuations are filtered. Runoff correlograms of the floods 2 and 3 also decrease very quickly which means that the watershed have a very short impulse response. In other words, the floods 2 and 3 are typical flash-floods events for which direct runoff is the main contribution to surface flows. At the opposite, the flood 10 exhibits a high inertia process which reflects a baseflow contribution to surface flows (Fig. 3-3); the time structure of the rainfall is totally modified by the watershed. The flood 9 shows an intermediate situation where direct runoff is followed by a baseflow contribution to surface flows.

The R_{up}/Q_1 cross correlograms of the floods 2, 3 and 9 exhibit sharp peaks between 1.75 h and 2.5 h, which characterises the direct response of the upstream watershed to runoff. Moreover, the cross correlogram of the flood 9 (Fig. 3-5) gives a good image of the R/Q transfer function of the watershed since the rainfall can be considered as a random process (Fig. 3-1); a breakpoint for a lag around 3.4 h (Fig. 3-5, see arrow) reflects a transition between direct runoff and delayed flows (baseflow). Secondary peaks for floods 2 and 3 are only due to the time structure of the rainfall (Fig. 3-1). The cross correlogram of the flood 10 shows a more delayed and damped response with two maxima; the first one corresponds to the direct response to runoff while the second one may be related both to the time structure of the rainfall (Fig. 3-1) and to delayed flows (baseflow).

- Fig. 3-2, Fig. 3-4 and Fig. 3-6 show results of auto-and cross correlations for the group B:

Structures of rainfall time series are much more complex for the group B (Fig. 3-2) than for the group A (Fig. 3-1); some rainfall correlograms show medium to long term trends (floods 1, 5 and 6, Fig. 3-2) which are due to longer rainfall events with relatively constant intensities. Q_1 correlograms decrease slowly and short term rainfall fluctuations are totally filtered by the watershed (Fig. 3-4). Rainfall cannot be interpreted as a random process since numerous non negligible peaks appear on R_{up} correlograms (Fig. 3-2). As a result, R_{up}/Q_1 cross correlograms give distorted images of the transfer function (Fig. 3-6). A response time around 4h can however be given (see arrows, Fig. 3-6), which is significantly higher than the mean watershed response time evaluated for the group A. The transfer is thus more influenced by delayed flows.

The watershed response time vary between 1.75 h and 6 h according to various hydrologic states of the watershed (initial soil moisture) and the rainfall intensities: both of them control the type of response: direct runoff and/or baseflow. Flash-floods show quick, short and sharp direct response to runoff, approximately 2 h after the rainfall, while delayed responses accounting for baseflow processes are predominant 3 h to 4 h after the rainfall. Small differences in time response may also be due to the spatial distribution of the rainfall since R_{up} is estimated using 1 rain gauge only.

The same study is now done in Q_2 (Fig. 2) to describe the hydrologic behaviour of the River downstream from the karst aquifer.

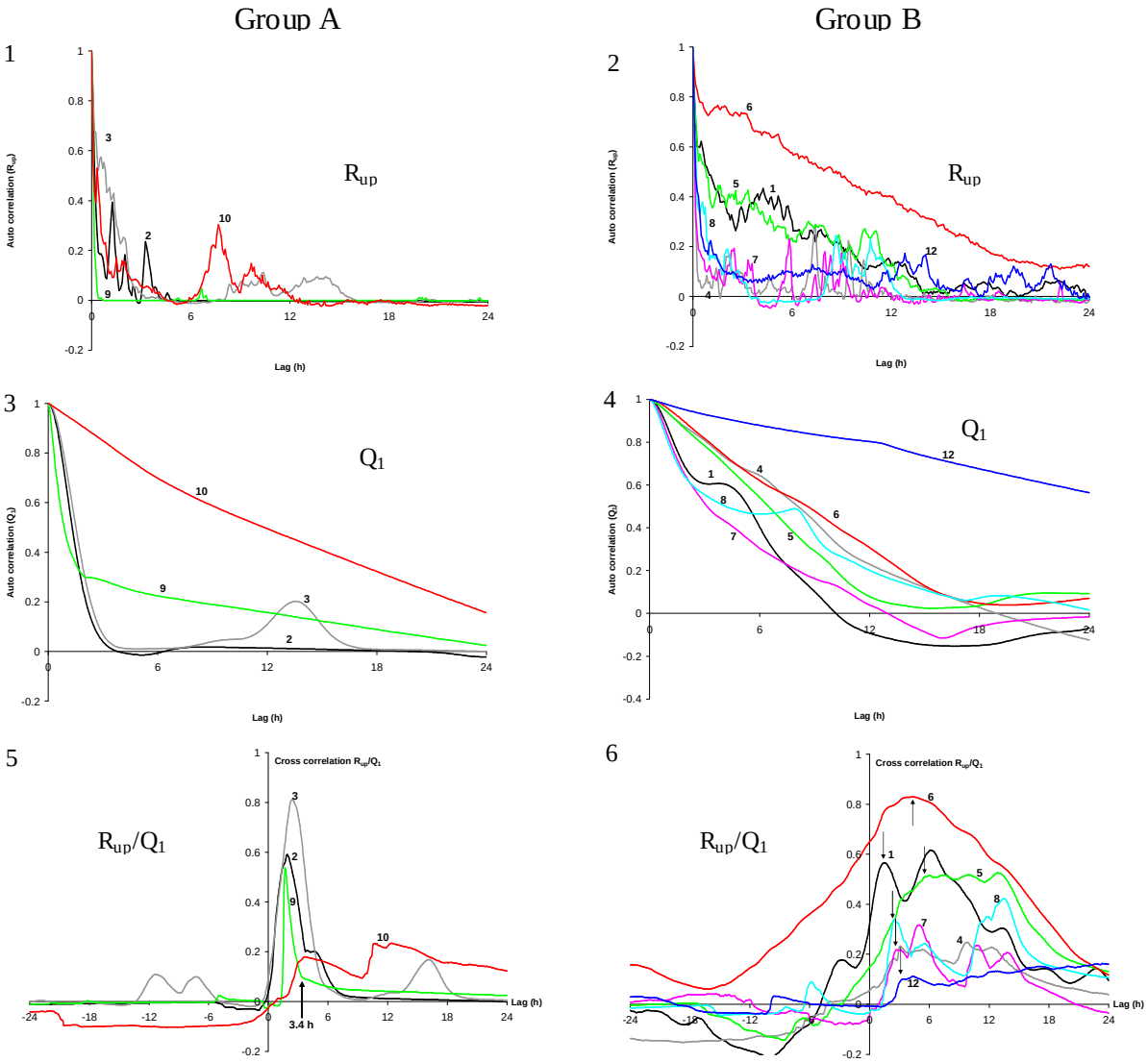

Fig. 3: Rup/Q_1 auto and cross correlograms, k=5 min, m=24 h, group A (left) and B (right).

R_{down}/Q_2 relationship

- Fig. 4-1, Fig. 4-3 and Fig. 4-5 show results of auto and cross correlations for the group A.

R_{down} correlograms are quite similar to those using R_{up} time series, and the same conclusion can be given. As a result, the time structure of the rainfall is fairly the same in all rain gauges and a strong modification of the discharge time structure between Q_1 and Q_2 reflects a change of the transfer function on the karst aquifer.

Q_2 correlograms (Fig. 4-3) shows that floods 2, 3 and 11 only characterises direct runoff (flash-flood), while the floods 9 and 10 are influenced by delayed flows coming from the upstream watershed and/or the karst aquifer. Moreover, both Fig. 3-3 and Fig. 4-3 show a second peak for the flood 3 at the same time lag (around 14 h), but this second peak is much higher using Q_2 time series. It means that bimodal flood transfer upstream and downstream from the karst aquifer is different. Flash flood transfer is well described by the R_{down}/Q_2 cross-correlogram (Fig. 4-7, floods 2, 3 and especially 11). The major difference between cross correlograms R_{up}/Q_1 of the flood 9 and R_{down}/Q_2 of the flood 11 is that no distinction between direct and delayed responses to runoff appears downstream from the karst aquifer (Q_2). Thus, no baseflow influences the floods transfer of the group A, which is in accordance with the losing reach definition (Table 1). Local runoff on karst thalwegs are furthermore responsible for a quick response (flood 10, arrow), as well as subsurface flows for delayed response (flood 9, arrow),

but runoff coefficients are very low for these two latter floods (Table 1). It means that surface flows are discontinuous between Q_1 and Q_2; the transfer is thus totally different since it only reflects low and local overland flows.

- Fig. 4-2, Fig. 4-4 and Fig. 4-6 show results of auto and cross correlations for the group B.

R_{down} correlograms are also quite similar to those using R_{up} time series, and the same conclusion can be given. Q_2 correlograms (Fig. 4-4) of the floods 1, 4, 5 and 6 show however higher auto correlation than Q_1 correlograms (Fig. 3-4) with relatively low slopes (strong inertia) while the floods 7, 8 and 12 show lower auto correlation. This can be partly related to the type of Karst/River exchange since the river during the floods 1, 5 and 6 has been described as a gaining reach in Table 1.

R_{down}/Q_2 cross correlograms (Fig. 4-6) show that the flood genesis is complex and results from various processes. The R_{down}/Q_2 cross correlogram of the flood 7 reflects direct runoff (sharp peaks) which was not highlighted by R_{up}/Q_1 cross correlogram (Fig. 4-6). As a result direct runoff also occurs between Q_1 and Q_2 due to a tributary of the River which flows on a partly non-karst watershed (Fig. 2) The others cross correlograms show maximum values for various lags (arrows) and the response time cannot be estimated.

R/Q auto and cross correlation analyses show that the karst aquifer controls the surface flow transfer by modifying the flood wave; karst contribution to surface flows particularly influences the medium to long term hydrologic response (>12 h, low slopes of R_{down}/Q_2 cross correlogram) while stream losses reduce the direct response to runoff (R_{up}/Q_1).

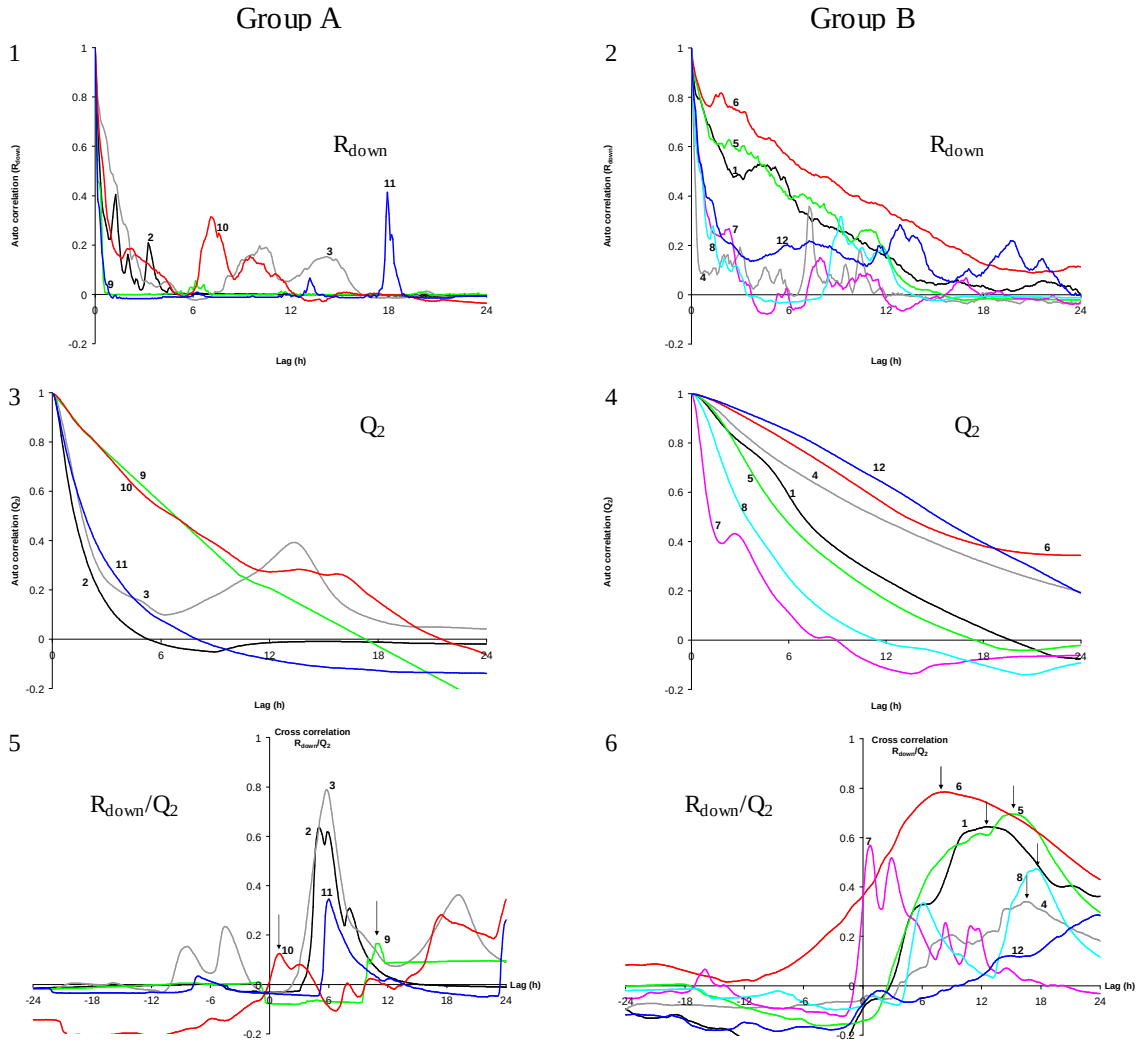

Fig. 4: R_{down}/Q_2 auto and cross correlograms, k=5 min, m=24 h, group A (left) and B (right).

Q_1/Q_2 relationship

In the time domain: Only cross correlograms are computed (Fig. 5-1 and Fig. 5-2) since Q_1 and Q_2 auto correlograms have already been computed (Fig. 3-3, Fig. 3-4, Fig. 4-3 and Fig. 4-4).

Cross correlograms of the group A allow describing flash-floods transfer; Q_1/Q_2 cross correlation is strong for the floods 2, 3 and 11 (acf close to 0.9) when the time lag is between 5 h and 6 h (Fig. 5-3). Cross correlograms are furthermore very sharp and quite symmetrical with high slopes which means that flood wave modification is low (low diffusion) and that the kinematic wave approximation could be used for the flood routing modelling. Results of the floods 9 and 10 are not used since surface flows were discontinuous between Q_1 and Q_2 (local runoff and subsurface flows in Q_2 without relation with Q_1).

Cross correlograms of the group B also show high correlations but the time structures are totally different. The cross correlogram of the flood 7 is a particular case which shows a maximum for a negative time lag; it means that the flood is recorded in Q_2 and then in Q_1 (direct runoff between Q_1 and Q_2). As a result, a high cross correlation does not always reflect the real flood routing since the two time series are influenced by a third one (rainfall). The other cross correlograms (Fig. 5-4) are complex with maximum peak between 3 h (flood 6) and 6 h (flood 4). Secondary peaks appear for lag around 8 h to 12 h (floods 1, 8 and 12) but they only reflect the time structure of the rainfall (Fig. 3-1, Fig. 3-2, Fig. 4-1 and Fig. 4-2). Low decrease of cross correlogram means that the transfer is more diffuse for the group B. Non negligible cross correlations for negative time lags (Fig. 5-2) show that other inputs influence the transfer of delayed flows: lateral karst inflows and/or subsurface flows.

As a result, the transfer time between Q_1 and Q_2 is estimated between 3 h and 6 h. A 3 h to 4 h transfer time characterises the flood routing through the karst aquifer while slower transfers account for lateral karst inflows.

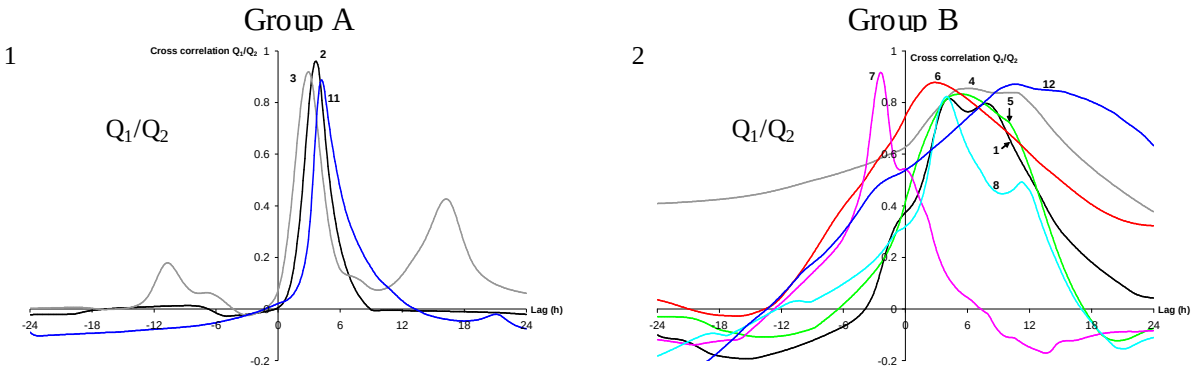

Fig. 5: Q_1/Q_2 cross correlograms, k=5min, m=24h, group A (left) and B (right).

In the frequency domain: Bode gain and phase plots are given in Fig. 6 for the floods 2, 5 and 6. During theses floods, the River between Q_1 and Q_2 has been identified as losing, variably gaining/losing and gaining reach respectively. Differenced time series have been used to enhance the frequency response estimate by removing long term trends in PSD estimates. Frequency to time (period) conversion is given on the top of each graph (grey dashed lines, Fig. 6). A 95% confidence interval (black dashed lines, Fig. 6) is given according to Eq. 13 both for gain and phase estimates.

The frequency response computed with the flood 5 (Fig. 6) show a very large confidence interval which results from low values of K^2_{12} (12), especially for long term components; it means that the system does not respect the LTI assumption and few information can be obtain by this approach. The system is indeed strongly time variant and non-linear since the river behaves alternatively as a losing or as a gaining reach during the flood routing.

The River was a losing reach during the flood 2 (Table 1) for which the gain and phase (Fig. 6) estimates are accurate. Low and medium frequencies ($f<1.1\ 10^{-4}$, $T>2.5h$) are attenuated ($G<0dB$) while some short-term variations are greatly amplified (Fig. 6, flood 2). It means that the karst aquifer

behaves as a component of the Karst/River system which store surface water and, moreover, that storage and the Q_1 time series are linearly dependent. The frequency response estimate shows a single resonant frequency at 1.9 10^{-4}Hz (1,4h, Fig. 6) which is interpreted as the exceeding of the infiltration rate through the karst drainage network for successive flood peaks. In other words it means that if a second flood peak occurs at least 3 h after the first one, the ‘‘memory’’ of the previous flood is low, while if the flood peaks are closer, the system becomes critical since the response of the system is still influenced by the previous flood peak (Bailly-Comte et al., 2008b). These results are shown in a synthetic way in Fig. 7a.

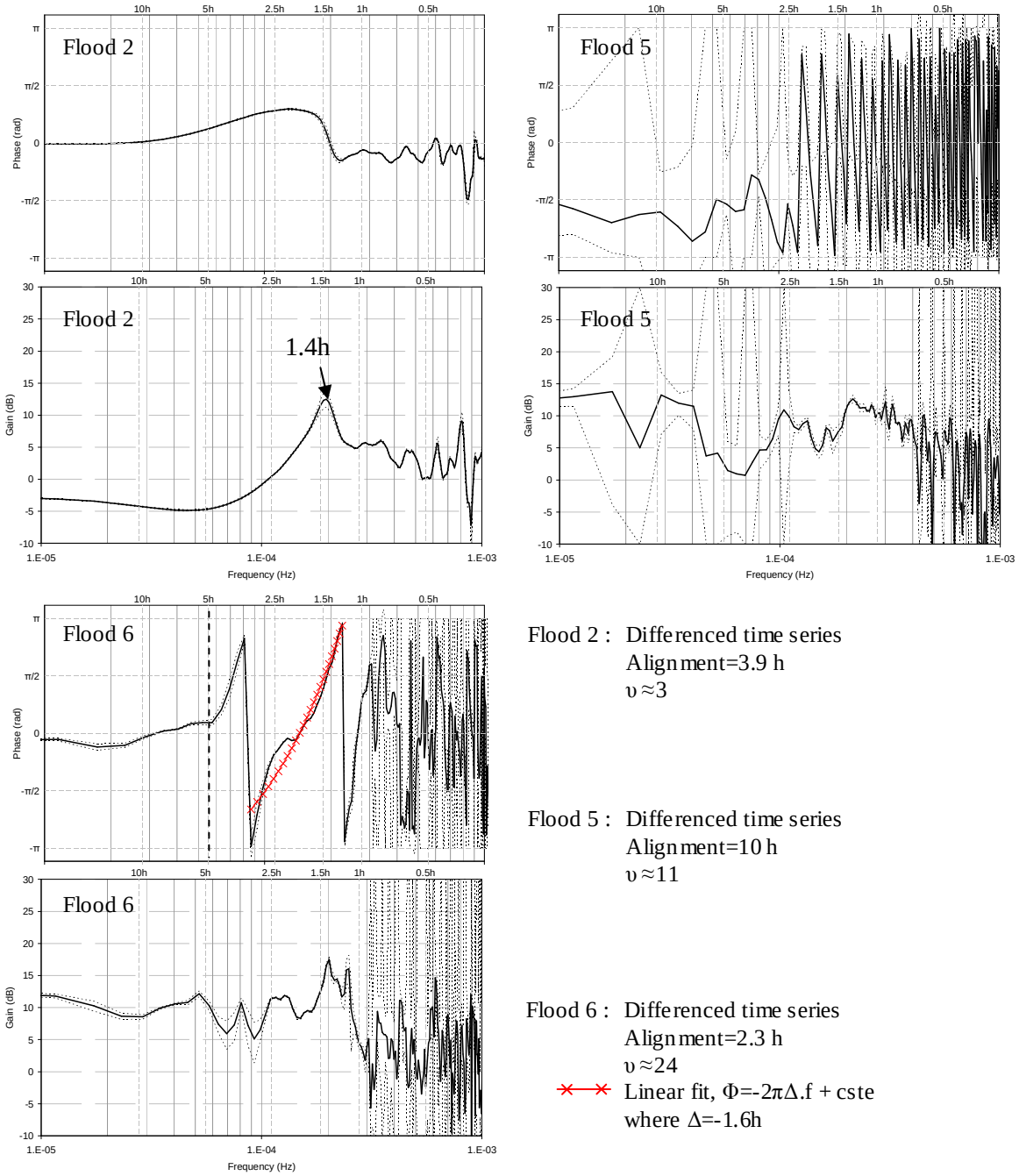

Fig. 6: Q_1/Q_2 frequency response function using both aligned and differenced data, k=5min, m=24h, floods 2, 5, and 6; black dashed lines represent the 95% confidence interval.

At the opposite, the River was a perfect gaining reach during the flood 6 (Table 1) since direct runoff in Q_1 and karst discharge between Q_1 and Q_2 were simultaneously recorded (Bailly-Comte et al.,

2008b). Bode plots show that Q_1 is amplified both for low and high frequencies. It means that the karst aquifer behaves as a component of the Karst/River system which enhances the surface flows at short and long term and that karst contribution to surface flows and the Q_1 time series are linearly dependent. Phase functions computed with aligned data is close to 0 for periods higher than 5 h (Fig. 6, flood 6). It means that the modification of long term components in the input signal is the predominant process which explains the transfer time. A phase delay is estimated by a linear fit using (9) for shorter period. The phase delay is about -1.6 h (phase advance) for period shorter than 2.5 h (Fig. 6, see the solid line). Thus, short and long term modifications reflect two different processes with different transfer time that are the surface flood routing (short term) and delayed karst lateral inflows (long term), as shown in a synthetic way in Fig. 7b.

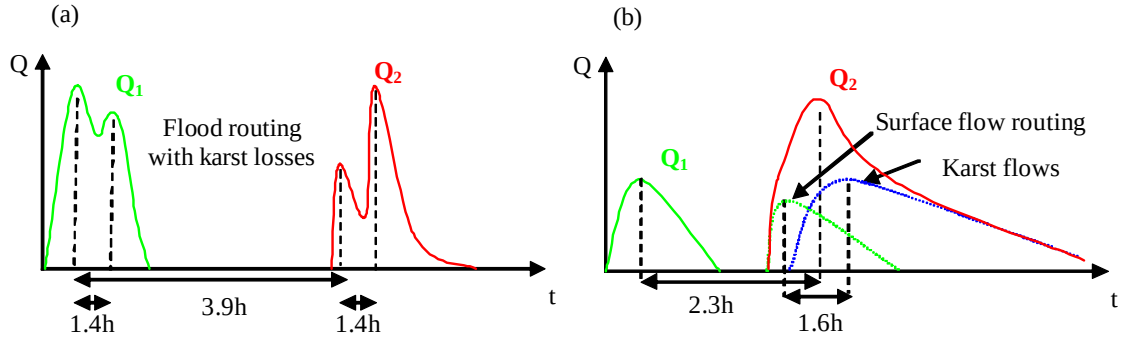

Synthetic representation of the flood transfer in case of a losing stream and very low initial water table in the karst aquifer.

Synthetic representation of the flood transfer in case of a gaining stream and very high initial water table in the karst aquifer.

Fig. 7: Flood routing in case of losing or gaining stream through the karst aquifer.

V. Conclusion

The R/Q studies show that a direct response to runoff occurs around 2 h after the rainfall in Q_1 and 5 to 6 h after the rainfall in Q_2. The baseflow contribution to runoff hydrograph becomes predominant 3 h after the rainfall in Q_1, but little information may be given for delayed flows in Q_2 by the R/Q relationship. The karst aquifer has to be considered as a strongly time-variant component of the Karst/River that does not allow assessing the response time of the watershed.

Further information is provided by the study of the Q_1/Q_2 relationship. It shows that the flood routing may be described as a transformation of the Q_1 time series through a LTI system if the River behaves as a losing or as a gaining reach. Bode plot is a suitable data analysis tool for transfer functions description since it highlights the various phenomena which occur on different time scale: surface flow routing from Q_1 to Q_2, exceeding of the infiltration rate through the karst drainage network and karst contribution to surface flows. All these results are useful to characterize the flood genesis in the karst watershed in case of a losing or a gaining reach but are not sufficient in case of an alternatively losing/gaining reach since complex (non-linear) interactions with the aquifer modify the flood routing.

It is thus shown that flood genesis and routing through a karst watershed cannot be simulated by a simple convolution system; LTI assumptions may however be valid if the stream is only a losing or a gaining stream. These two cases are precisely the cases for which the floods are the highest. These floods occur either in autumn in very low water table condition in the aquifer due to a very high cumulative and strong intensity rainfall event or in winter in very high water table conditions in the karst aquifer due to a strong karst contribution to surface flows. Time series analysis may thus provide useful results which allow understanding the hydrologic response of a complex watershed and enhancing hydrologic modelling and the flood forecast.

References

Bailly-Comte, V., 2008. Interactions hydrodynamiques entre les eaux de surface et les eaux souterraines en milieu karstique. Doctorat Thesis, Université Montpellier 2.

Bailly-Comte, V., Jourde, H., Roesch, A. and Pistre, S., 2008a. Mediterranean flash flood transfer through karstic area. Environmental Geology, 54(3): 605-614.

Bailly-Comte, V., Jourde, H., Roesch, A., Pistre, S. and Batiot-Guilhe, C., 2008b. Time series analyses for Karst/River interactions assessment: Case of the Coulazou river (southern France). Journal of Hydrology, 349(1-2): 98-114.

Box, G.E.P., Jenkins, G.M. and Reinsel, G.C., 1994. Time series analysis, Forecasting and Control, Third Edition. Prentice-Hall, Inc., 598 pp.

Denic-Jukic, V. and Jukic, D., 2003. Composite transfer functions for karst aquifers. Journal of Hydrology, 274(1-4): 80-94.

Dreiss, S.J., 1983. Linear unit-response functions as indicators of recharge areas for large karst springs. Journal of Hydrology, 61(1-3): 31-44.

Jenkins, G.M. and Watts, D.G., 1968. Spectral Analyses and Its Applications. Holden-Day, San Francisco, 525 pp.

Jourde, H., Roesch, A., Guinot, V. and Bailly-Comte, V., 2007. Dynamics and contribution of karst groundwater to surface flow during Mediterranean flood. Environmental Geology, 51(5): 725-730.

Jukic, D. and Denic-Jukic, V., 2004. A frequency domain approach to groundwater recharge estimation in karst. Journal of Hydrology, 289(1-4): 95-110.

Jukic, D. and Denic-Jukic, V., 2006. Nonlinear kernel functions for karst aquifers. Journal of Hydrology, 328(1-2): 360-374.

Labat, D., Ababou, R. and Mangin, A., 2000a. Rainfall-runoff relations for karstic springs. Part I: convolution and spectral analyses. Journal of Hydrology, 238(3-4): 123-148.

Labat, D., Ababou, R. and Mangin, A., 2000b. Rainfall-runoff relations for karstic springs. Part II: continuous wavelet and discrete orthogonal multiresolution analyses. Journal of Hydrology, 238(3-4): 149-178.

Larocque, M., Mangin, A., Razack, M. and Banton, O., 1998. Contribution of correlation and spectral analyses to the regional study of a large karst aquifer (Charente, France). Journal of Hydrology, 205(3-4): 217-231.

Long, A.J. and Derickson, R.G., 1999. Linear systems analysis in a karst aquifer. Journal of Hydrology, 219(3-4): 206-217.

Mangin, A., 1984. Pour une meilleure connaissance des systemes hydrologiques a partir des analyses correlatoire et spectrale. Journal of Hydrology, 67(1-4): 25-43.

Massei, N., Dupont, J.P., Mahler, B.J., Laignel, B., Fournier, M., Valdes, D. and Ogier, S., 2006. Investigating transport properties and turbidity dynamics of a karst aquifer using correlation, spectral, and wavelet analyses. Journal of Hydrology, 329(1-2): 244-257.

Padilla, A. and Pulido-Bosch, A., 1995. Study of hydrographs of karstic aquifers by means of correlation and cross-spectral analysis. Journal of Hydrology, 168(1-4): 73-89.

Rahnemaei, M., Zare, M., Nematollahi, A.R. and Sedghi, H., 2005. Application of spectral analysis of daily water level and spring discharge hydrographs data for comparing physical characteristics of karstic aquifers. Journal of Hydrology, 311(1-4): 106-116.

Yevjevich, V., 1972. Stochastic processes in hydrology. Water resources publications, Fort Collins, Colorado, USA, 276 pp.